1-9-2013

Hydrophobic Hydrogel Caged H_3PO_4 as a New Class of High-Temperature Proton Exchange Membranes with Enhanced Acid Retention

Qunwei Tang

Guoging Qian
University of South Carolina - Columbia, guoqing@mailbox.sc.edu

Kevin Huang
University of South Carolina - Columbia, huang46@cec.sc.edu

Publication Info

Published in *RSC Advances*, Volume 3, Issue 11, 2013, pages 3520-3525.

RSC Advances

RSC Publishing

COMMUNICATION

View Article Online
View Journal | View Issue

Hydrophobic hydrogel caged H_3PO_4 as a new class of high-temperature proton exchange membranes with enhanced acid retention†

Cite this: *RSC Advances*, 2013, **3**, 3520

Received 11th July 2012,
Accepted 21st December 2012

DOI: 10.1039/c3ra21417f

www.rsc.org/advances

Qunwei Tang,[a] Guoqing Qian[b] and Kevin Huang*[a]

We herein report a new class of high-temperature proton exchange membranes comprised of poly(acrylic acid-*graft*-hexadecyltrimethylammonium bromide) (PAA-*g*-CTAB) or poly (acrylic acid)-*graft*-poly(ethylene glycol) (PAA-*g*-PEG) hydrophobic hydrogel caged H_3PO_4. The membranes exhibit reasonable proton conductivity, enhanced H_3PO_4 retention ability and low solubility in water, making them promising as potential high performance and robust electrolytes for high-temperature proton exchange membrane fuel cells. Although the proton conductivity is still lower than that of H_3PO_4 doped PBI membranes, the new concept provides a different approach to proton exchange membranes for acid retention.

1 Introduction

Significant advances in Nafion-based proton exchange membrane fuel cells (PEMFCs) have been achieved in the past few decades[1] with a growing number of pre-commercial demonstration units being deployed for both transportation and stationary power generation applications. The eventual commercialization of the technology as an economically viable product is, however, still hampered by the cost and reliability of the overall system, the root cause of which is largely associated with unsatisfactory performance in materials and operations.[2] One global research effort undertaken in recent years to address the issue is to operate PEMFCs at a temperature higher than 100 °C, preferably in the range of 100–200 °C. Many benefits can be gained for a PEMFC by operating in this temperature range: enhanced tolerance to CO and H_2S, elimination of water management, the ability to use non-precious metals as the electrodes,[3] and promoted electrode kinetics and ionic conductivity. The enabling material for high-temperature PEMFCs is the proton exchange membrane (PEM) that needs to be stable and proton conducting at 100–200 °C and in anhydrous conditions.[4] The leading high-temperature PEMs are the H_3PO_4 doped poly(benzimidazole) (PBI) membrane series, among which, that developed by Benicewicz *et al.* using a sol–gel hydrolysis process with poly(phosphoric acid) has shown the best performance.[5] However, one of the issues associated with H_3PO_4-doped PBI membranes is the gradual leaching-out of the H_3PO_4 from PBI membrane by the moisture formed at the cathode during long-term operation of fuel cell.[2] To reduce the loss of H_3PO_4, hydrophobic H_3PO_4 derivatives have been proposed as dopants for PBI membranes. Ma has doped PBI membranes with H_3PO_4, monophenylphosphoric acid, diphenylphosphoric acid, and sulfophenylphosphoric acid, showing a significant improvement in acid retention from diphenylphosphoric acid doped PBI membrane.[6] However, the proton conductivity of these membranes is too low ($\sim 10^{-4}$ S cm^{-1}) for their practical application in PEMFCs.

Here we demonstrate the use of hydrophobic poly(acrylic acid-*graft*-hexadecyltrimethylammonium bromide) (PAA-*g*-CTAB) and poly(acrylic acid)-*graft*-poly(ethylene glycol) (PAA-*g*-PEG) hydrogels as placeholders to contain the proton conducting H_3PO_4 phase in a new class of PEM for high-temperature PEMFCs. The design of these new membranes is inspired by the structure of the well-known Nafion PEM where the backbone of the Nafion polymer possesses extreme hydrophobicity, while its terminal sulfonic acid functional group shows extreme hydrophilicity. In the presence of water, the hydrophilic sulfonic acid domains become highly hydrated to provide high proton conductivity while the hydrophobic Nafion polymer backbone provides good mechanical stability for the membrane. In the new PEMs reported, the hydrophobic PAA-*g*-CTAB and PAA-*g*-PEG polymers provide mechanical support for proton conducting H_3PO_4 for high-temperature PEMFC applications. The synthesized PAA-*g*-CTAB and PAA-*g*-PEG hydrogels are chemically crosslinked polymers with a highly interconnected 3D framework, allowing a large amount of alcohol assisted H_3PO_4 accommodation. Once incorporated into the microstructure, the functional H_3PO_4 can be permanently caged inside the network, yielding excellent H_3PO_4 retention ability even under high compression.

[a]*Department of Mechanical Engineering, University of South Carolina, Columbia, SC 29201, United States. E-mail: HUANG46@cec.sc.edu*

[b]*Department of Chemistry, University of South Carolina, Columbia, SC 29208, United States*

† Electronic supplementary information (ESI) available. See DOI: 10.1039/c3ra21417f

2 Experimental

Synthesis of hydrophobic PAA-*g*-CTAB composites

The hydrophobic PAA-*g*-CTAB composites were synthesized according to a simple two-step method which has been described in our previous work.[7–10] In detail,[11] a solution mixture consisting of acrylic acid monomer (99.5%, extra pure, Acros Organics), CTAB (⩾=99% min., Acros Organics) and crosslinker *N*,*N*′-(dimethylene)acrylamide (NMBA, 96%) was made by agitating deionized water (10 mL), acrylic acid (10 g), CTAB (0.5 g) and NMBA (0.004 g) in a water-bath at 85 °C. Under vigorous stirring, ammonium persulfate (APS, 98%) (0.045 g) was added to the above mixture. The acrylic acid monomers were initiated by the thermal decomposition of APS to form PAA prepolymers. The viscosity increased gradually as polymerization proceeded. When the viscosity of the PAA prepolymers reached around 180 mPa s^{-1} (the viscosity of the reagent was measured using a Haaker ReoStress RS75 rheometer at a shear rate of around 100 s^{-1}), the reagent was poured into a petri dish and cooled to room temperature until the formation of a transparent elastic gel. The PAA-*g*-CTAB membranes were then molded into ϕ 3 cm die. After washing with ethanol, the membranes were dried under vacuum at 50 °C for 24 h.

Synthesis of the hydrophobic PAA-*g*-PEG composite

The hydrophobic PAA-*g*-PEG composite was also synthesized according to the method described in our previous work.[7–10] In detail, a solution mixture consisting of acrylic acid monomer, PEG (M_w = 20 000, Acros Organics) and crosslinker NMBA was made by agitating DI-water (10 mL), acrylic acid (10 g), PEG (2.5 g) and NMBA (0.004 g) in a water-bath at 85 °C.[10] Under vigorous stirring, 0.045 g of APS was added to the above mixture. When the viscosity of the PAA prepolymers reached around 180 mPa s^{-1}, the reagent was poured into a petri dish and cooled to room temperature until the formation of an elastic transparent gel. The PAA-*g*-PEG membranes were then molded into ϕ 3 cm die. After washing with ethanol, the membranes were dried under vacuum at 50 °C for 24 h.

Preparation of hydrophobic hydrogel caged H_3PO_4 membranes

The dried PAA-*g*-CTAB or PAA-*g*-PEG membranes were immersed in H_3PO_4 ethanol alcohol solutions with concentrations of 10 and 30 wt%. The absorption process was carried out in a sealed bottle at room temperature for 7 days until the weight of the membrane hydrogels reached a constant for an absorption equilibrium. The resultant product was then rinsed with DI water and dried under vacuum at 60 °C for 3 days to drive off all ethanol and obtain the final PAA-*g*-CTAB caged H_3PO_4 and PAA-*g*-PEG caged H_3PO_4 membranes. The H_3PO_4 loading (wt%) shown in Table 1 was calculated by:

$$H_3PO_4 \text{ loading (wt\%)} = \frac{m_{PA} - m_0}{m_{PA}} \quad (1)$$

where m_{PA} (g) is the mass of PAA-*g*-CTAB caged H_3PO_4 or PAA-*g*-PEG caged H_3PO_4 and m_0 (g) is the mass of PAA-*g*-CTAB or PAA-*g*-PEG.

Electrochemical characterization

The through-plane proton conductivities of the hydrophobic membranes in the dried state were characterized with ac-impedance spectroscopy using a Zahner IM6 Electrochemical Workstation (ZAHNER-Electrik Gmbh & Co., Kronach, Germany) in a frequency range of 1 Hz–4 MHz and an ac amplitude of 10 mV in a temperature range of 25–183 °C. Self-adhesive carbon conductive tapes with a diameter of 1.18 cm were used as the electrodes. The ohmic resistance associated with the membranes was determined from the high frequency intersection of the spectrum with the Z′ axis, from which the proton conductivity can be calculated.

H_3PO_4 retention

The H_3PO_4 retention was evaluated by both cumulative H_3PO_4 release and residual proton conductivity. 0.2 g of PAA-*g*-CTAB caged H_3PO_4 or PAA-*g*-PEG caged H_3PO_4 sample was immersed in 50 mL DI-water under vigorous agitation. The samples were taken out and then immersed in 50 mL of fresh DI-water at an interval of one hour. The amount of H_3PO_4 release in DI-water was measured using *Standard Methods for the Examination of Water and Wastewater* 4500-P E (ascorbic acid method), which can determine the concentration of *o*-phosphate-P in the range of 0.01 to 2 mg L^{-1} (ppm). The cumulative H_3PO_4 release from both PAA-*g*-CTAB caged H_3PO_4 and PAA-*g*-PEG caged H_3PO_4 was determined on a Shimadzu UV-2450 UV-vis-NIR spectroscope at room temperature by measuring the absorbance at 880 nm. A standard curve of Abs = 3.327[P] (R = 0.998) was recorded before measuring. The residual conductivity of the membranes at 183 °C was measured with a Zahner IM6 Electrochemical Workstation.

Other characterization

The morphologies of the samples were captured with a Zeiss Ultra Plus field emission scanning electron microscope (FESEM). Swollen PAA-*g*-CTAB caged H_3PO_4 or swollen PAA-*g*-PEG caged H_3PO_4 membranes were cut into ultrathin films and kept at freezing temperature to remove the ethanol.

3 Results and discussion

The synthesis of hydrophobic PAA-*g*-CTAB and PAA-*g*-PEG hydrogels is an example of a free-radical initiated grafting copolymer-

Table 1 H_3PO_4 loadings in PAA-*g*-CTAB caged H_3PO_4 and PAA-*g*-PEG caged H_3PO_4 membranes

Concentration of H_3PO_4 alcohol solution (wt%)	H_3PO_4 loadings in PAA-*g*-CTAB (wt%)	H_3PO_4 loading in PAA-*g*-PEG (wt%)
10	71.2	30.2
30	68.8	49.7

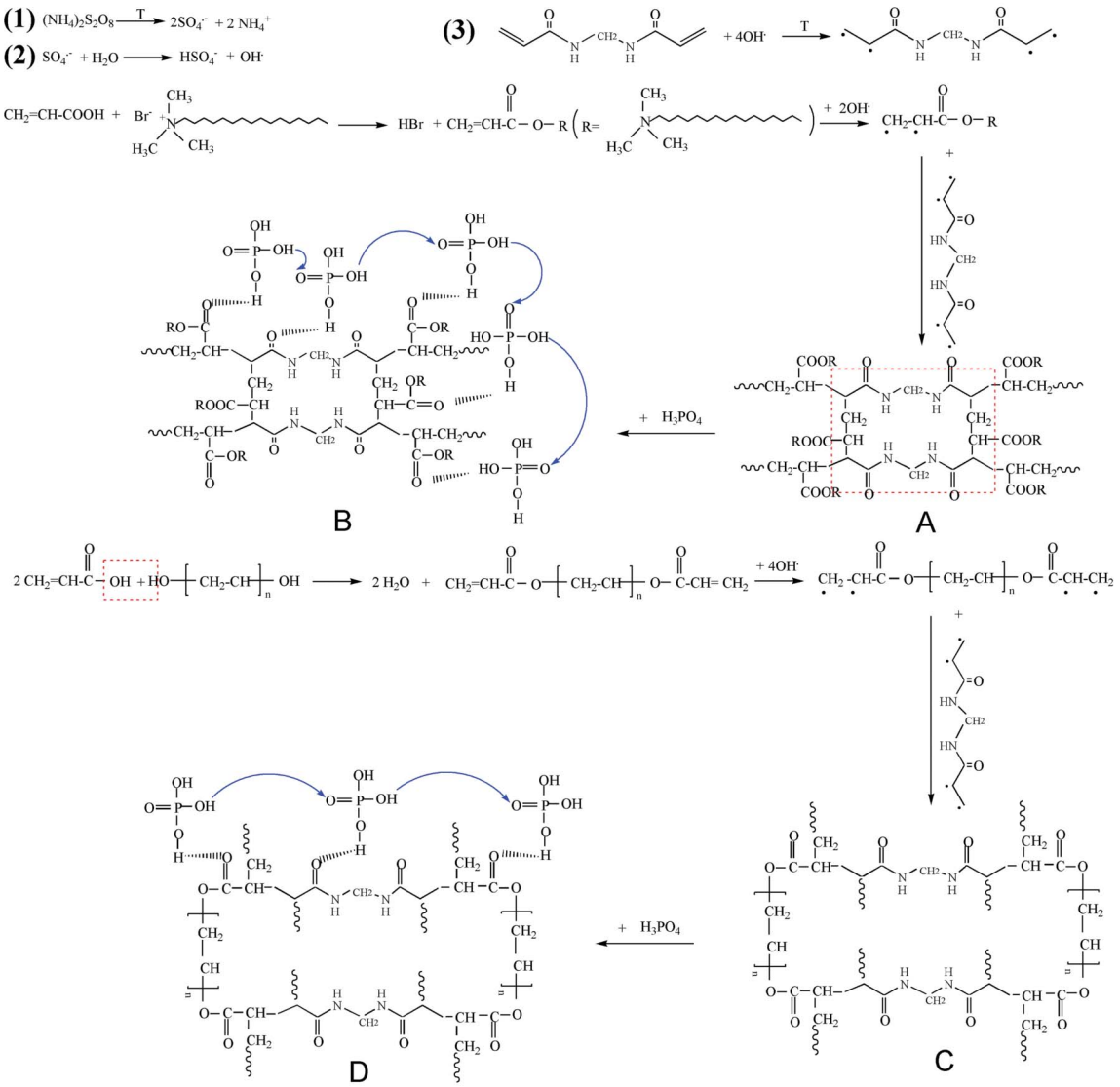

Fig. 1 Schematic of the synthesis routes of PAA-*g*-CTAB and PAA-*g*-PEG hydrophobic hydrogel materials by an aqueous solution polymerization route. The molecular structures are given to show the 3D frameworks of PAA-*g*-CTAB and PAA-*g*-PEG.

ization process (Fig. 1), a detailed description of which can be found in the Experimental section. Ammonium persulfate (APS) is used as the thermal initiator for the polymerization. Homolytic cleavage of each peroxide bond (–O–O–) in the APS provides two $SO_4^{\cdot-}$ radical anions [reaction (1) in Fig. 1], which react with water to form the hydroxyl radical ($OH^{\cdot}$) [reaction (2) in Fig. 1].[12,13] The $OH^{\cdot}$ radicals serve as the initiator for the process of polymerization by generating free radicals on the >C=C< bonds of *N*,*N*′-(dimethylene)acrylamide (NMBA) and acrylic acid [reaction (3) in Fig. 1]. In the mixture of acrylic acid and CTAB, they form a complex and release one molecule of HBr because of the strong electrostatic attraction between a negatively charged acrylic acid molecule and a positively charged CTAB molecule.[14] However, the acrylic acid molecule and PEG form one macromolecular monomer by dehydrating one water molecule.[12] During chain propagation, the acrylic acid-CTAB and acrylic acid-PEG will form 3D network-structured PAA-*g*-CTAB (Structure A in Fig. 1) and PAA-*g*-PEG (Structure C in Fig. 1) frameworks, respectively, because of the biradical nature of NMBA.[15] The grafting of CTAB or PEG on poly(acrylic acid) (PAA) backbones results in the loss of hydrophilicity from PAA and the creation of hydrophobicity from the long alkyl chains in the newly formed PAA-*g*-CTAB and PAA-*g*-PEG. In fact, the as-obtained PAA-*g*-CTAB is the integration of complicated structures comprising 3D PAA, linear PAA, 3D PAA-*g*-CTAB and linear CTAB. Similarly, the resultant PAA-*g*-PEG is composed of 3D PAA, linear PAA, 3D PAA-*g*-PEG and linear PEG. Physical entanglement in combination with the chemical bonds and hydrogen bonds results in the formation of a high-strength composite. The as-synthesized PAA-*g*-CTAB and PAA-*g*-PEG composites are typical hydrophobic hydrogel materials that can swell in H_3PO_4 alcohol solution (*al*-H_3PO_4), resulting in an open pore structure allowing for easy incorporation of H_3PO_4 into the 3D

frameworks, driven by osmotic pressure present across the membranes.[16] The absorption of *al*-H_3PO_4 by PAA-*g*-CTAB and PAA-*g*-PEG polymers causes the hydrophobic frameworks to stretch and expand considerably in volume, the process of which can be briefly summarized by the following three steps:[17] (i) adsorption of alcohol on the surface of hydrophobic PAA-*g*-CTAB or PAA-*g*-PEG membrane because of the hydrophobicity of long alkyl chains; (ii) relaxation of PAA-*g*-CTAB and PAA-*g*-PEG macromolecule chains, and (iii) stretch of the whole PAA-*g*-CTAB and PAA-*g*-PEG macromolecule chains in *al*-H_3PO_4. After the removal of the alcohol, the PAA-*g*-CTAB caged H_3PO_4 (Structure B in Fig. 1) and PAA-*g*-PEG caged H_3PO_4 (Structure D in Fig. 1) are successfully synthesized, and the remaining H_3PO_4 molecules in the vicinity of PAA-*g*-CTAB and PAA-*g*-PEG framework backbones form hydrogen bonds with C=O and O–H groups. The H_3PO_4 away from the framework backbones is free. We observed that the sample with low H_3PO_4 loading exhibited rigidity, but it became more flexible at higher H_3PO_4 loading, indicating the presence of free H_3PO_4 within the membranes. The free H_3PO_4 plays an important role in achieving the high proton conductivity of the membranes.

The cross-sectional microstructures of the as-synthesized anhydrous PAA-*g*-CTAB and PAA-*g*-PEG polymers are shown in Fig. 2a and c, respectively, the microstructures of which are highly dense with no open pores. After imbibing in *al*-H_3PO_4 and drying at 60 °C, the membranes shrink to a large degree and become dense as shown in Fig. 2b and d. At this stage, the caged H_3PO_4 molecules have formed hydrogen bonds with the functional groups, such as O–H and C=O, abundant in the polymer framework of PAA-*g*-CTAB and PAA-*g*-PEG, or established their own 3D conduction pathways *via* hydrogen bonds. The protons can then migrate along these connected hydrogen bonds throughout the membrane by successive proton transfer and reorientation steps schematically shown in Fig. 1b and d.[18] Revealed by the freeze-drying technique, the internal open porous frameworks of PAA-*g*-CTAB and PAA-*g*-PEG memebranes have a layered laminar structure with interconnected channels in between for PAA-*g*-CTAB caged H_3PO_4 and a randomly porous structure for PAA-*g*-PEG caged H_3PO_4.

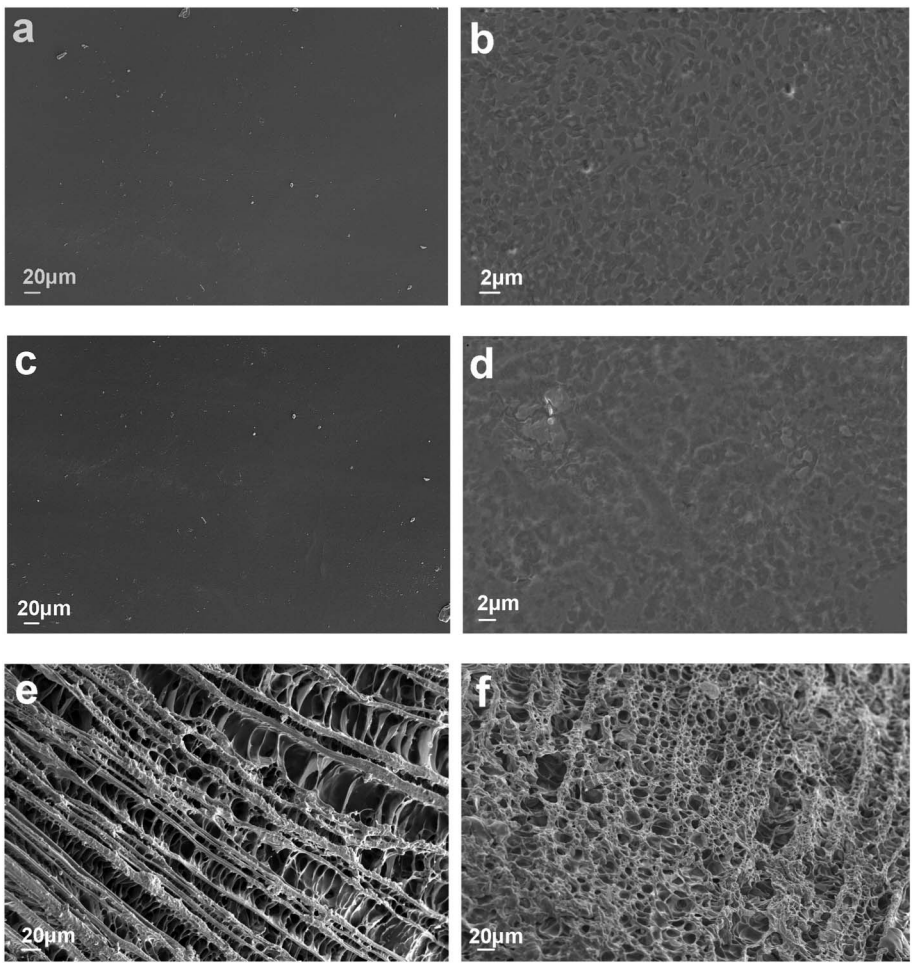

Fig. 2 Cross-sectional view of microstructures of (a) as-synthesized PAA-*g*-CTAB polymer, (b) PAA-*g*-CTAB caged H_3PO_4 (H_3PO_4 loading: 71.2 wt%) membrane dried at 60 °C, (c) as-synthesized PAA-*g*-PEG polymer, (d) PAA-*g*-PEG caged H_3PO_4 (H_3PO_4 loading: 49.7 wt%) memberane dried at 60 °C. Images (e) and (f) are the 3D porous framworks of hydrophobic PAA-*g*-CTAB and PAA-*g*-PEG hydrogel caged H_3PO_4 membranes revealed by freeze-drying off alcohol from the membranes, respectively.

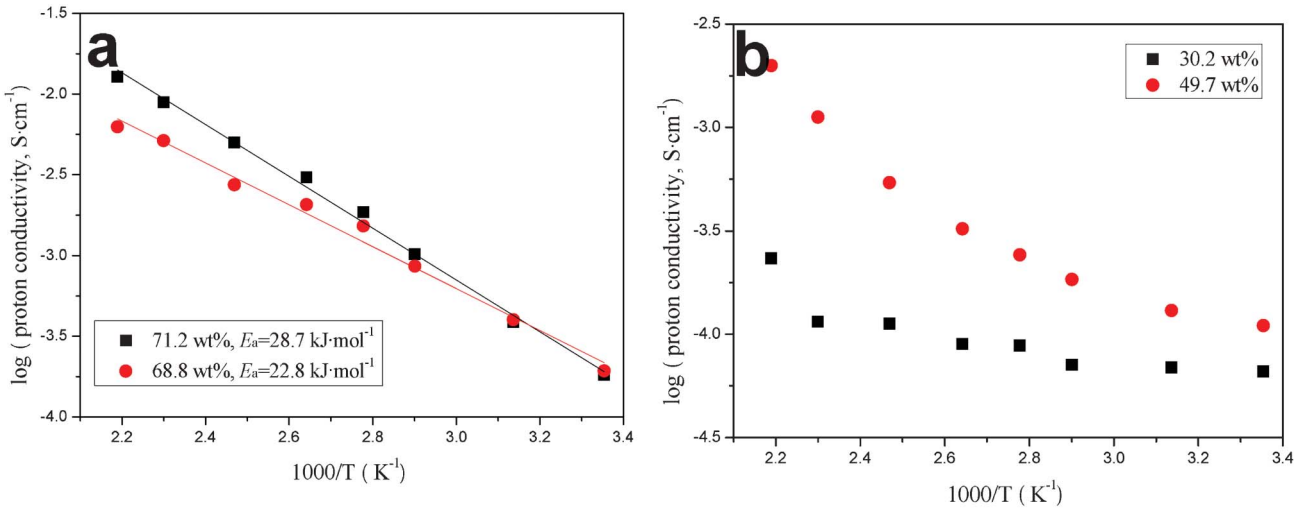

Fig. 3 (a) Arrhenius plots of proton conductivity of PAA-*g*-CTAB caged H_3PO_4 and (b) the conductivity–temperature characteristics of PAA-*g*-PEG caged H_3PO_4 membrane measured under anhydrous conditions.

The proton conductivities of PAA-*g*-CTAB membranes with two H_3PO_4 loadings measured under dry air from 25–183 °C follow reasonably the Arrhenius relationship in Fig. 3a. It is interesting to note that the activation energy in this membrane, E_a, appears to increase with H_3PO_4 loading; this is opposite to that of H_3PO_4-doped PBI membranes,[2] but similar to that of linear polyacrylamide–H_3PO_4 membranes.[19] Although it is unclear as to the exact mechanism of proton conduction in such a composite organic–inorganic membrane,[20–22] the exhibited E_a reflects a combined effect from proton transport *via* hydrogen bonds present in H_3PO_4 as well as those formed with the host's functional group, C=O, in the polymer as shown in Fig. 1B. However, the proton conductivity of H_3PO_4-imbibed PAA-*g*-PEG, Fig. 3b, follows neither the Arrhenius relationship [$\sigma = A\exp(-E_a/kT)$] nor the Vogel–Tammann–Fulcher relationship (VTF) $\{\sigma(T) = AT^{-1/2}\exp[-E_a(T - T_0)]\}$.[23] This unusual conductivity behaviour is not well understood at this point.

To evaluate the H_3PO_4 retention ability of the hydrophobic membranes in the presence of water, PAA-*g*-CTAB caged H_3PO_4 (with 71.2 wt% H_3PO_4 loading) and PAA-*g*-PEG caged H_3PO_4 (with 49.7 wt% H_3PO_4) membranes were immersed into 50 mL DI-water. The cumulative H_3PO_4 dissolution was subsequently measured using *Standard Methods for the Examination of Water and Wastewater* 4500-P E (ascorbic acid method). After water exposure, the conductivity of the membranes was measured again at 183 °C. The release behaviour of H_3PO_4 from the hydrophobic membranes is shown in Fig. S1, ESI.† Overall, the level of H_3PO_4 release is insignificant and decreased after 5 h, indicating a good H_3PO_4 retention ability in the presence of water. To further understand the release mechanism of H_3PO_4, the accumulative

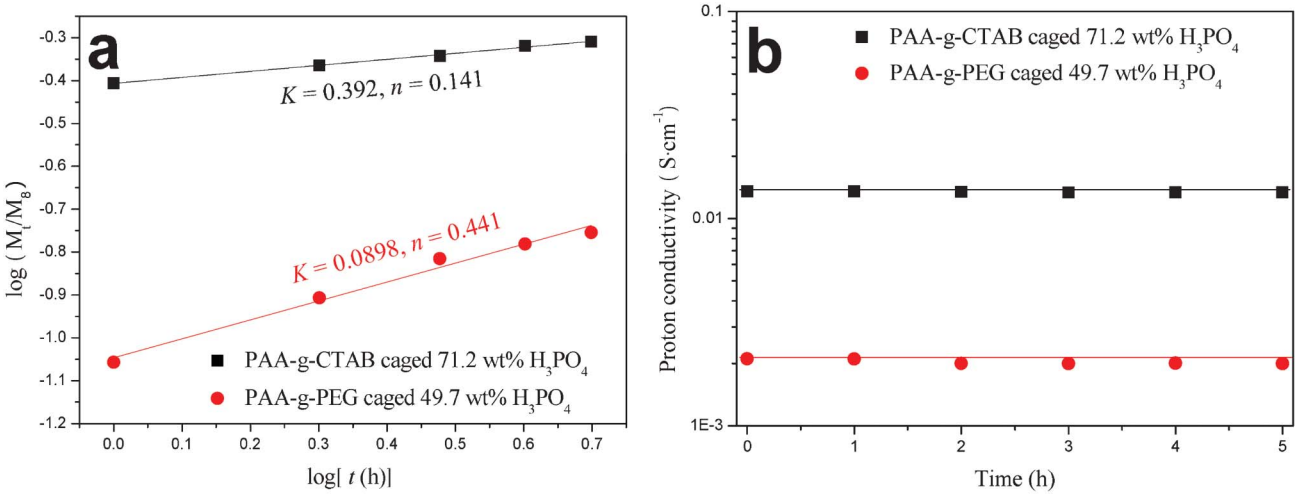

Fig. 4 (a) The plot of $\log(M_t/M_\infty)$ *versus* $\log(t)$ and (b) residual proton conductivity of PAA-*g*-CTAB caged H_3PO_4 (H_3PO_4 loading: 71.2 wt%) and PAA-*g*-PEG caged H_3PO_4 (H_3PO_4 loading: 49.7 wt%) membranes after H_3PO_4 release treatment. The proton conductivity was measured under dry air and at 183 °C.

H_3PO_4 release mass is studied by using the semi-empirical equation $M_t/M_\infty = kt^n$,[24] where M_t and M_∞ are the cumulative mass of the H_3PO_4 release at time t and at equilibrium, respectively; k is the rate constant relating to the property of the hydrophobic matrix; n is the release exponent depicting the transport mechanism. By plotting $\log(M_t/M_\infty)$ *versus* $\log(t)$, the n and k values were obtained from the fitting and are shown in Fig. 4a. The k value from PAA-*g*-CTAB caged H_3PO_4 is 0.392, higher than that from PAA-*g*-PEG caged H_3PO_4, $k = 0.0898$. This difference can be attributed to the formation of a denser framework with a higher H_3PO_4 loading,[25] which in turn slows down the release of hydrogen-bonded H_3PO_4. In addition, the n values in both cases were found to be in the range of 0 to 0.5, implying a pseudo-Fickian diffusion release mechanism.[24] Overall, the rate of H_3PO_4 release in these hydrophobic membranes is negligible compared to that of H_3PO_4-doped PBI membranes where H_3PO_4 can be totally leached out in the presence of water in less than 10 min.[5] The high acid retention ability has also been confirmed by the unchanged proton conductivities of the membranes shown in Fig. 4b, measured after water exposure. Clearly, this acid retention is a benefit of the formation of an external and hydrophobic layer on the surface of the membranes during the drying process.[26] The hydrophobic repulsion on the membrane surface is strong enough to stop water molecules from attacking H_3PO_4 caged in the membrane due to the zero osmotic pressure.[15]

4 Conclusions

In summary, a new class of PEMs consisting of hydrophobic PAA-*g*-CTAB and PAA-*g*-PEG polymers imbibed with H_3PO_4 has been synthesized by a simple and low-cost approach as potential high-temperature PEMs. The H_3PO_4 molecules are caged inside the 3D polymeric framework after drying, effectively mitigating the loss of H_3PO_4. Proton conduction is carried out by hydrogen bonds in H_3PO_4 as well as those formed between H^+ in H_3PO_4 and functional groups, C=O or O–H, in the hydrophobic polymer matrix. Proton conductivities of 0.0128 and 0.00199 S cm^{-1} at 183 °C under anhydrous host's conditions have been achieved for PAA-*g*-CTAB caged H_3PO_4 (at H_3PO_4 loading: 71.2 wt%) and PAA-*g*-PEG caged H_3PO_4 (at H_3PO_4 loading: 49.7 wt%), respectively. Although the proton conductivity is still lower than the reported values of H_3PO_4 doped PBI, the new hydrophobic PEMs show significantly enhanced H_3PO_4 retention ability in the presence of water. More importantly, the idea to use 3D hydrophobic hydrogel materials as the templates to imbibe intrinsic proton conductors can be applied to other systems with higher hydrophobicity and organic solvent absorbency to promote higher H_3PO_4 loading, and therefore proton conductivity for low-cost and robust high temperature PEMs.

Acknowledgements

The authors gratefully acknowledge the University of South Carolina for providing Seedling Fund to this project. The authors also thank Prof. Brian C. Benicewicz, Prof. Chuanbing Tang and Dr Kejian Yao for suggestive comments and helping process samples for SEM observation.

References

1 T. H. Yu, Y. Sha, W. G. Liu, B. V. Merinov, P. Shirvanian and W. A. Goddard III, *J. Am. Chem. Soc.*, 2011, **133**, 19857.
2 J. A. Asensio, E.M. Sanchez and P. Gomez-Romero, *Chem. Soc. Rev.*, 2010, **39**, 3210.
3 C. Ke, J. Li, X. Li, Z. Shao and B. Yi, *RSC Adv.*, 2012, **2**, 8953.
4 S. Y. Lee, A. Ogawa, M. Kanno, H. Nakamoto, T. Yasuda and M. Watanabe, *J. Am. Chem. Soc.*, 2010, **132**, 9764.
5 L. Xiao, H. Zhang, E. Scanlon, L. S. Ramanathan, E. W. Choe, D. Rogers, T. Apple and B. C. Benicewicz, *Chem. Mater.*, 2005, **17**, 5328.
6 Y. Ma, *PhD Thesis*, Case Western Reserve University, 2004.
7 Q. W. Tang, X. M. Sun, Q. H. Li, J. H. Wu and J. M. Lin, *J. Colloid Interface Sci.*, 2009, **339**, 45.
8 Q. W. Tang, X. M. Sun, Q. H. Li, J. H. Wu and J. M. Lin, *Colloids Surf., A*, 2009, **346**, 91.
9 J. M. Lin, Q. W. Tang, D. Hu, X. M. Sun, Q. H. Li and J. H. Wu, *Colloids Surf., A*, 2009, **346**, 177.
10 Q. W. Tang, X. M. Sun, Q. H. Li, J. H. Wu and J. M. Lin, *Sci. Technol. Adv. Mater.*, 2009, **10**, 015002.
11 Z. Y. Tang, Q. Liu, Q. W. Tang, J. H. Wu, J. L. Wang, S. H. Chen, C. Cheng, H. Yu, Z. Lan, J. Lin and M. Huang, *Electrochim. Acta*, 2011, **58**, 52.
12 N. A. Ibrahim, A. Amr, B. M. Eid, Z. E. Mohamed and H. M. Fahmy, *Carbohydr. Polym.*, 2012, **89**, 648.
13 B. Singh and V. Sharma, *Int. J. Pharm.*, 2010, **389**, 94.
14 J. H. Wu, Q. W. Tang, H. Sun, J. M. Lin, H. Y. Ao, M. L. Huang and Y. F. Huang, *Langmuir*, 2008, **24**, 4800.
15 Q. H. Li, J. H. Wu, Z. Y. Tang, Y. M. Xiao, M. L. Huang and J. M. Lin, *Electrochim. Acta*, 2010, **55**, 2777.
16 R. Luo and H. Li, *Acta Biomater.*, 2009, **5**, 2920.
17 D. J. Enscore, H. B. Hopfraberg and V. T. Stannett, *Polymer*, 1977, **18**, 793.
18 K. D. Kreuer, *Solid State Ionics*, 2000, **136–137**, 149.
19 D. Rodriguez, C. Jegat, O. Trinquet, J. Grondin and J. C. Lassègues, *Solid State Ionics*, 1993, **61**, 195.
20 Q. W. Tang, G. Q. Qian and K. Huang, *RSC Adv.*, 2012, **2**, 10238.
21 Q. W. Tang, S. S. Yuan and H. Y. Cai, *J. Mater. Chem. A*, 2013, **1**, 630.
22 Q. W. Tang, H. Y. Cai, S. S. Yuan, X. Wang and W. Q. Yuan, *Int. J. Hydrogen Energy*, 2013, **38**, 1016.
23 J. H. Wu, S. Hao, Z. Lan, J. Lin, M. Huang, Y. Huang, L. Fang, S. Yin and T. Sato, *Adv. Funct. Mater.*, 2007, **17**, 2645.
24 N. W. Franson and N. A. Peppas, *J. Appl. Polym. Sci.*, 1983, **28**, 1299.
25 D. Ma, K. Tu and L. M. Zhang, *Biomacromolecules*, 2010, **11**, 2204.
26 I. Bravo-Osuna, C. Ferrero and M. R. Jimenez-Castellanos, *Eur. J. Pharm. Biopharm.*, 2005, **59**, 537.